

Received September 14, 2020, accepted September 21, 2020, date of publication October 23, 2020, date of current version November 3, 2020.

Digital Object Identifier 10.1109/ACCESS.2020.3033300

Design of Archimedes Spiral Antenna to Optimize for Partial Discharge Detection of Inverter Fed Motor Insulation

PENG WANG¹, SHIJIN MA¹, SHAKEEL AKRAM^{1,2}, (Member, IEEE),
KAI ZHOU¹, (Member, IEEE), YIDONG CHEN¹, AND MUHAMMAD TARIQ NAZIR³

¹College of Electrical Engineering, Sichuan University, Chengdu 610065, China

²UMR 5214, CNRS, Institut d'Electronique et des Systemes (IES), Université de Montpellier, 34000 Montpellier, France

³School of Mechanical and Manufacturing Engineering, University of New South Wales, Sydney, NSW 2052, Australia

Corresponding author: Shakeel Akram (shakeel.akram@scu.edu.cn)


This work was supported by the National Natural Science Foundation of China under Grant 51977134.

ABSTRACT The partial discharge (PD) in inverter-fed motors generated from high frequency and short rise time impulsive voltage are more complex than traditional sinusoidal voltage operated motors due to the noise initiated from fast switching power electronics devices. Available PD sensors and related technology for DC and sinusoidal voltage cannot be used at repetitive impulsive voltage conditions. This work aims to report the design of antenna with optimized geometry and satisfied parameters to detect PD for impulsive voltage. The antenna is verified and the influence of both impulse voltage parameters and test configuration on PD features are discussed. The envelope detection technique after the filter in the frequency domain was proposed to reduce the complexity and cost of PD test hardware under impulsive voltages with fast rise times. The frequency domain energy of PD from motor insulation is mainly distributed in the range of 0.6-1.8 GHz. By increasing the amplitude and frequency of input impulsive voltage, the range of PD energy spectrum is enlarged to (1.5-1.8 GHz) and by decreasing input amplitude the PD signal strength decays abruptly. Moreover, the high-frequency distribution of PD energy attenuates more severely with the distance and the electromagnetic energy of PD decays nonlinearly with the increase of propagation distance. Therefore, under the premise of satisfying the safety test, selecting the test distance below 15 cm can ensure that the test results have a high signal-to-noise ratio and signal integrity. The experience reported in this study could provide suggestions for off-line PD measurements for inverter-fed motor insulation evaluations for manufacturers.

INDEX TERMS Inverters, motors, UHF antennas, partial discharges, impulse voltage.

I. INTRODUCTION

Power electronics have been becoming the hidden technology driving the world. Advance and the most successful application of power electronics is the propulsion motor of electric drive systems for transportation facilities such as high-speed trains, new energy vehicles and electrical ships. After connected to converters, the conventional 3-phase inductive machine can obtain excellent performance such as energy-saving, easy speed regulation and soft start. Therefore, these fast switching inverter-fed motors are getting popularity and replacing conventional AC motors.

The associate editor coordinating the review of this manuscript and approving it for publication was Christopher H. T. Lee .

Different from traditional motors fed by sinusoidal and DC voltages, the invert-fed motor is subjected to high-frequency impulse voltage waveform from pulse-width modulation voltage converters. The impulse train will stress the stator and bring more challenges to the insulation systems of machines. There have been several reports on the failure of inverter-fed motors [1]–[4]. Subsequently, the reliability problems of inverter-fed motors have brought more and more attention to industries.

It has been acknowledged that the over-voltage at the machine's stator terminal resulted from the impedance mismatch between the stator and connecting cables is the main reason for inverter-fed motor failure, as shown in Figure 1 [1], [5]. Longer cable and higher dv/dt will induce higher over-voltages at the motor stator terminals. In addition, the

overvoltage at the terminal will distribute unevenly in the windings of stators and, thus, enhance the electric field in the local area of insulation systems. If partial discharge inception voltage (PDIV) is lower than the electric field of the insulation system, PD activities can happen with high possibility and accelerate the electrical ageing of insulation systems, leading to the final failure of the insulation [6], [7]. The impact of PD events on the insulation should be discussed considering inverter-fed motors with different rated voltage and insulation systems. PD is not allowed in random wounded low voltage inverter-fed motor in its whole lifetime, as insulation breakdown can occur within a short period as a result of eroded insulation because of PD in case of low-voltage inverter-fed motors whose random wounded insulation is made up of organic materials [8]. Therefore, the off-line PD inception voltage (PDIV) should be carried out and the obtained PDIV values will be compared with the rated voltage of the motor to optimize the insulation design to make sure that the working voltage is lower than PDIV to avoid PD events during all the lifetime. For high-voltage inverter-fed motors with form-wounded winding insulation constituted of inorganic materials (e.g., mica) with corona resistance performance, moderate PD events are allowed. However, if the insulation working voltage is higher than PDIV, i.e., PD activities occur in the insulation, the lifetime (endurance) of the insulation should meet the design requirement (e.g., 20 years). Therefore, the PDIV is also a critical parameter for the insulation and the endurance under voltage higher than PDIV (e.g., 1.5 to 3.0 times PDIV) should be conducted to evaluate its lifetime.

In the recent 20 years, the International Electrotechnical Commission (IEC) has been working on building related standards for the tests to increase the insulation reliability of inverter-fed motors. As stipulated in the IEC 60034-18-41 and IEC 60034-18-42, PDIV and endurance life tests that are recommended respectively for the insulation systems of low-voltage random- and form-wounded winding insulation systems of inverter-fed motors [9], [10]. It can be summarized that the PDIV is a critical parameter that can reflect the insulation performance for both low-voltage and high-voltage inverter-fed motors. The off-line PD measurements have, therefore, become a crucial technique when assessing the performance of insulation systems working at the impulse voltages produced by power electronics.

Compare with the relatively mature PD test technologies under sinusoidal and DC voltages, careful consideration is required when using impulsive voltages with fast rise time to perform PD tests as it incurs more difficulties. Firstly, the interference induced by power electronics switches (ns to μ s level) can generate intensive disturbance, overlaps with PD signals in time and frequency domain. The shorter the rise time (i.e., faster switching of power electronics devices), the more interference will be obtained when performing PD tests. The PD and interference can overlap in both time and frequency domain, which are very difficult to distinguish PD from disturbance due to the switching of power devices.

In addition, the increasing voltage slew rate and frequency from the power electronics devices made up of new generation wide band gap semiconductor (SiC, GaN) bring more difficulties to the PD test under impulsive voltages because the converter designed using wideband gap power devices can generate repetitive impulse voltages with a frequency higher than 1 MHz and rise time shorter than 20 ns [11].

Secondly, PD tests under the impulsive voltages become more complicated because of test sensitivity and influence that impulse voltage parameters have on PD features. During the PDIV tests, the first and most important consideration is to choose appropriate repetitive voltages generators that can produce stress like these coming from the converters. The impulsive voltage used for off-line PDIV tests has more complex voltage parameters such as rise time, fall time, frequency and duty cycles, in general, only frequency and magnitude can be changed when performing PDIV tests under sinusoidal voltages [12]. It has been reported that the impulse voltage parameters will have a significant impact on the PD features such as amplitude, phase, accumulated energy and time-frequency distribution [3], [13]–[17]. This indicates that while performing PD tests under impulsive voltages, the effect that impulsive voltage parameter has on PDIV measurement sensitivity must be considered.

One important consideration is to choose appropriate PD sensors when high sensitivity PD tests are performed using repetitive impulsive voltages. Although the coupling capacitor and high frequency current transformer (HFCT) are widely used for on-line and off-line PD test under sinusoidal voltages, the two types of sensors cannot be adopted anymore for PD tests using fast rise time impulsive voltage because their frequency response is too low to distinguish PD signal from the serious disturbance resulted from switching on & off of power electronics [18]–[20]. The optical test methods, such as photomultiplier (PMT), can be used for PD tests under noisy environmental conditions [21], [22]. However, PMT must be positioned close to the test object (i.e., < 5 cm) due to the rapid attenuation of optical signals and environmental noise, which limit the off-line and on-line application of PMT for performing PD test at impulsive voltages. The use of conventional coupling capacitance on PD tests at impulse voltages was also reported [23]. It is challenging to suppress the interference from the power electronics to obtain the required sensitivity, especially when impulsive voltage rise time is less than 100 ns.

It has been known that the ultra-high frequency (UHF) technique by using an antenna sensor is a potential approach for PD tests at impulsive voltages. This is because the UHF antenna can receive the high frequency electromagnetic energy generated by PD activities and the disturbance with lower frequency energy distribution can be removed efficiently by using high-pass filter [5], [24], [25]. However, almost all the antenna reported for PD tests under sinusoidal or DC voltages based on the conclusions that PD energy is mainly distributed within the frequency ranging from 0 GHz to 0.8 GHz [38]. We have reported that the PD generated

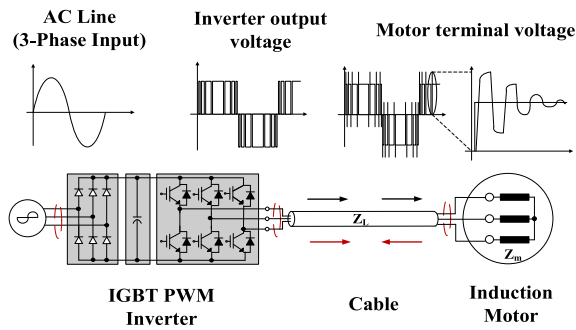


FIGURE 1. Sketch of phase-to-phase voltage at the terminals of a motor fed from a PWM inverter.

by 200 ns rise time repetitive impulse voltage has energy distribution substantially in frequency domain ranging from 0.8 to 2.0 GHz [26], [27], indicating that the conventional antenna used at sinusoidal voltages cannot be used anymore under the influence of the intensive disturbance due to switching activities of power devices to obtain satisfied signal to noise ratio (SNR). To the author’s knowledge, there are few reports on the antenna specially designed to conduct PD tests using fast rise times impulsive voltages.

Therefore, the main works of this study are firstly to design a novel Archimedes Spiral Antenna (ASA) with optimized parameters specially used for PDIV measurements of inverter-fed motor insulation at repetitive impulsive voltages with fast rise times resorting to geometry modeling and simulation technologies according to the PD energy distribution at repetitive impulsive voltages. Then to verify frequency response, sensitivity and SNR for a designed antenna, a PD test using repetitive impulsive voltages on the turn to turn insulation of inverter fed motors was performed. Moreover, the influence of the test parameters such as impulsive voltage frequency and antenna distance were investigated. In addition, the envelope technique used for reducing the sampling rate of hardware was discussed when using the UHF technique for on-line PD monitoring.

II. SELECTION, GEOMETRY MODELLING AND SIMULATION OF THE ANTENNA

A. PD AND DISTURBANCE FEATURES

Removing or suppressing the switching interference produced by power electronics devices to extract PD pulses with high SNR is a key technique for PD measurement using fast rise time impulsive voltages. To design a UHF antenna having high SNR specially used for performing impulsive voltages PD tests, the PD and disturbance feature analysis is firstly needed. Therefore, PD tests were conducted on crossed enameled wires made up of turn to turn insulation of low-voltage random winding inverter-fed motors. The repetitive impulsive voltages with 200 ns rise time and fall time, peak to peak voltage 2.5 kV and 50 % duty cycle were used for the tests [13]. The disturbance and the PD pulses were shown in Figure 2a. It can be seen that the switching disturbance with

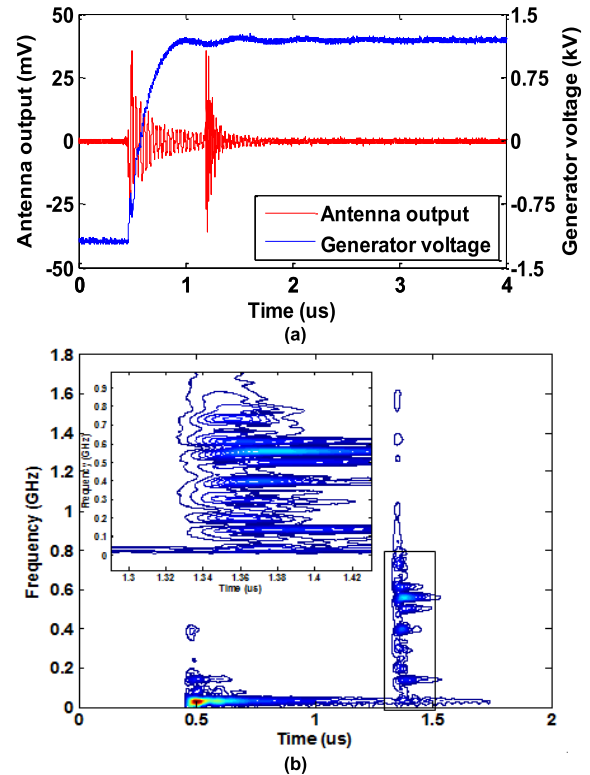


FIGURE 2. (a) PD and switching disturbance of power electronics (b) STFT result of the signal.

unchanged magnitude occurs at the rising flanks of impulse voltage waveform, while the PD pulse after the disturbance pulse has a similar magnitude with the disturbance. The short-time Fourier transform (STFT) results, reported in Figure 2b, shows that the spectral energy of the disturbance can span up to 500 MHz. Note that PD pulse has considerable energy distribution ranging from 0 to 1.8 GHz, indicating that, to enhance SNR while conducting PD test at impulsive voltages, the sensor needs to receive the PD energy in the frequency domain higher than 0.5 GHz [13].

The PD pulses and spectrum obtained at impulse (200 ns rise time and 50 % duty cycle) and sinusoidal voltages with 2.5 kV peak to peak magnitude and 50 Hz frequency are shown in Figure 3 [41]. Obviously, impulsive and sinusoidal voltages with same peak to peak magnitude and frequency give rise to PD pulses having different features in both time and frequency domains. PD pulses at impulse voltages have obvious energy distribution at frequency range higher than 500 MHz, while most PD energy at sinusoidal voltages distributes below 700 MHz. Accordingly, it can be drawn that, (1) PD tests antenna at sinusoidal voltage should have the best performance (frequency gain) below 1 GHz; (2) PD tests antenna at impulse voltage waveform with rising time shorter than 200 ns rise time must receive the PD energy within the range of 0.5 to 2.0 GHz and, at the same time, a high pass frequency filter with cutting frequency around 0.5 GHz can be used to remove the energy generated by the switching disturbance.

TABLE 1. Different types of antennas used for proposed application.

Reference	Antenna Type	Design Bandwidth (GHz)	Radiation Pattern	Gain(dB)	-10dB S11 Bandwidth (GHz)
This work	Archimedes Spiral Antenna	0.5-2	Unidirectional	$-2.6@f_{min}/12.0@f_{max}$	0.75-2
[29]	single-arm Archimedean spiral antenna	0.5-3	Bidirectional	Not presented	1.2-2.4
[30]	patch antenna	1.5-2	Bidirectional	Not presented	Not presented
[31]	Vivaldi antenna	2-3	Bidirectional	Not presented	1-2, 1.47, 2.68
[32]	Hilbert Antenna	0.3-1	Bidirectional	$-12.8@f_{min}/-1.0@f_{max}$	Not presented

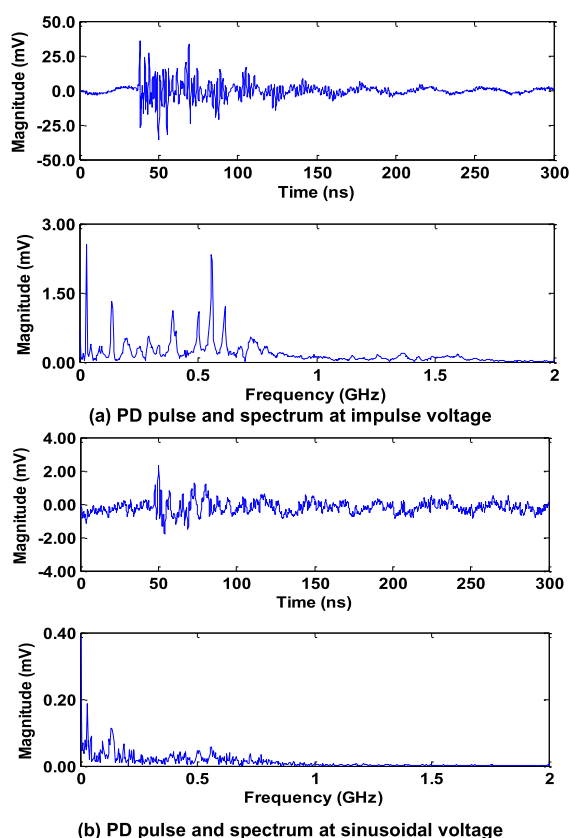


FIGURE 3. PD pulse and spectrum at impulse and sinusoidal voltages with same peak to peak magnitude and frequency.

B. ANTENNA SELECTION

Table 1 lists the different types of antenna used for the partial discharge detection of high voltage electrical insulation. Note that, although the Archimedean spiral antenna has been widely used in power systems at sinusoidal voltages, without impedance matching, the effective bandwidth of the single-arm Archimedean spiral antenna cannot meet requirements [28]. Affected by the nature of the antenna itself, the effective band range of the patch antenna is only distributed in 1.5-2 GHz [29]. The minimum frequency of Vivaldi antenna that can effectively receive discharge is 2 GHz, which is obviously higher than the minimum frequency of discharge

detection at repetitive impulsive voltage, and it is easy to lose more information in the frequency domain of discharge [30]. Hilbert Antenna have low gain and frequency domain bandwidth of less than 1 GHz, which are not suitable for the detection of PD at repetitive impulsive voltage [31]. Actually, the frequency domain of PD is mainly distributed in 0.5-2 GHz, so it is necessary to design UHF antenna with high gain, wide bandwidth, high directivity and appropriate size. The effective bandwidth refers to the impedance matching (return loss $S_{11} < -11$), higher gain and better directional performance within the designed bandwidth. To ensure the antenna can receive more part of the discharge signal. Considering that the Archimedes spiral antenna has been used for PD detection under traditional sinusoidal voltages in power systems for many years, we select this type of antenna and optimized its parameter to increase test sensitivity at fast impulsive voltages. For accurate detection of PD signal at impulse voltages, the tested object and antenna position were fixed, in other words, the PD signal from the object is directional. Therefore, the interference from other directions can be suppressed by adding a tapered reflecting cavity. In this way, the gain and the SNR is improved.

From the PD and disturbance test results, we can conclude that a broadband high frequency antenna (0.3-2 GHz sensor) is most suitable to receive electromagnetic signals excited by PD events at impulsive voltages [32]–[34]. And the existing UHF antenna used for PD tests at sinusoidal voltages cannot be directly applied to PD detection under impulse voltage conditions due to different frequency response requirements. The antenna must be specially designed considering the PD and switching disturbance features at impulse voltages.

Among all the antenna used for discharge measurements, Archimedes spiral antenna (ASA) with impedance matching unit advantages of good radiation performance in wideband [28]. An ASA has two spiral arms placed symmetrical embedded on a dielectric substrate, as shown in Figure 4. The spiral arm width is equivalent to the separation between the arms to obtain a self-integral structure whose impedance is independent of frequency.

To perform repetitive impulse voltage PD tests, the UHF sensors should have a good performance within frequency ranging from 0.5 to 2.0 GHz, where most energy of the PD

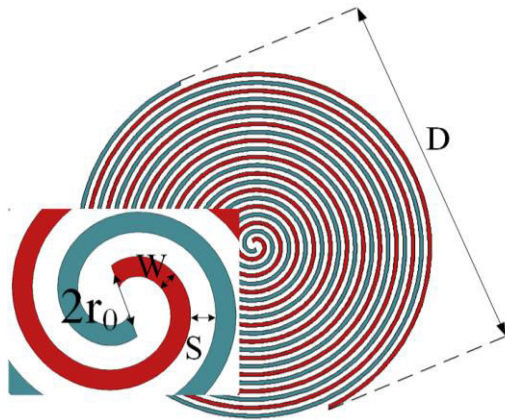


FIGURE 4. The structure of Archimedes spiral antenna.

induced by repetitive impulsive voltages distribute. It can therefore be obtained that the corresponding wavelength of this frequency range is 150~600 mm. An ASA can receive electromagnetic signals with a wavelength equal to the parameters of the antenna, as shown in Figure 4. The antenna diameter must meet the following requirements based on ASA principle [23],

$$2r_0 \leq \frac{\lambda_{\min}}{4} \tag{1}$$

$$\pi D \leq 1.25\lambda_{\max} \tag{2}$$

where r_0 , $2r_0$, λ_{\min} , λ_{\max} and D are the radial distance between the initial point and the center point of ASA, the distance between feeding points of two spiral arms, the wavelength is corresponding the lowest working frequency, the wavelength corresponding the highest working frequency and diameter of the effective area of the antenna, respectively. The ASA shown in Figure 4 has a symmetrical and balanced structure. When connecting the antenna to a receiver for most applications, a coaxial cable with an unbalanced feeding mode must be used. At the connection points of the antenna and the cable, the electromagnetic reflection will occur and cause substantial energy loss, which will reduce the signal to noise ratio, and would miss the small signals generated by the PD activities.

C. ANALYSIS OF VOLTAGE STANDING WAVE RATIO AND BALUN

Voltage standing wave ratio (VSWR) can evaluate the degree of impedance mismatching. It can be defined as the ratio between maximum radio frequency (RF) voltage to the minimum RF voltage along the transmission line. Higher VSWR means worse impedance matching between the antenna and coaxial feeder and thus, leads to more reflection energy at the interface. Therefore, the UHF sensor should have low VSWR (less than 2.0 in general) in the range of 0.5~2 GHz. The characteristic impedance of coaxial cable is used in this study is 50 Ω. The influence of the r_0 on the VSWR of the antenna is calculated on basis of the antenna structure reported in Figure 4 and the results are reported in Figure 5.

The characteristics impedance of ASA is generally higher than the coaxial cable. Consequently, the longer r_0 , the higher the impedance of the antenna, leading to higher degree impedance mismatching (see Figure 5) and thus, more energy loss due to wave reflection at the interface between the antenna and the connecting cable. Also, it can be concluded from the results in Figure 5 that lower VSWR than 2.0 cannot be achieved only by adjusting the distance between the antenna feed points.

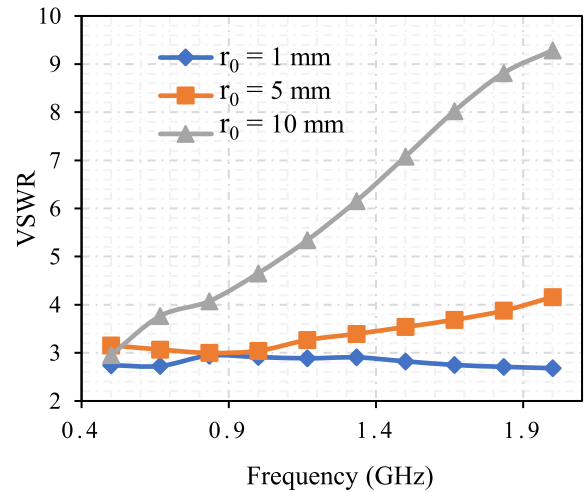


FIGURE 5. VSWR vs. the size of the Archimedes spiral antenna.

To reduce the energy loss between two parts, a match impedance device named Balun must be used. Also, Balun can play as a balanced-imbalance converter to ensure that two spiral arms have the same current distribution. The microstrips Balun designed for the antenna (see Figure 6a) has two exponentially graded microstrip and a dielectric that is parallelly placed on two surfaces of the substrate [35], [36]. To create balanced feed from the unbalanced, feed mode is unbalanced at port 2 and balanced at port 1. Consequently, after adding a Balun between the antenna and connection cable, the main parameters affect the VSWR are the distance between feeding points of two spiral arms (i.e., $2r_0$) and the geometry of the Port1 on the Balun (i.e., the width of port1, w_0). The influence of the width of port1, w_0 , on antenna's VSWR in the frequency domain was calculated, keeping r_0 at 1 mm.

The VSWR vs. frequency is shown in Figure 6b. Wider port1 will give rise to lower VSWR, in other words, better impedance matching. It can be seen in most areas of the frequency ranging from 0.5 to 2.0 GHz. The VSWR is lower than 2.0 when the w_0 is 1.0 mm, 1.4 mm and 1.6 mm. Note

that smoothing changing VSWR is needed to improve the performance of the designed antenna in the whole frequency range. Finally, 1.4 mm was selected as the port1 width considering the stability of VSWR.

D. THE RADIATION PATTERN AND GAIN

According to the above simulation results, the r_0 of the antenna and w_0 of the microstrips are set to 1.0 mm and

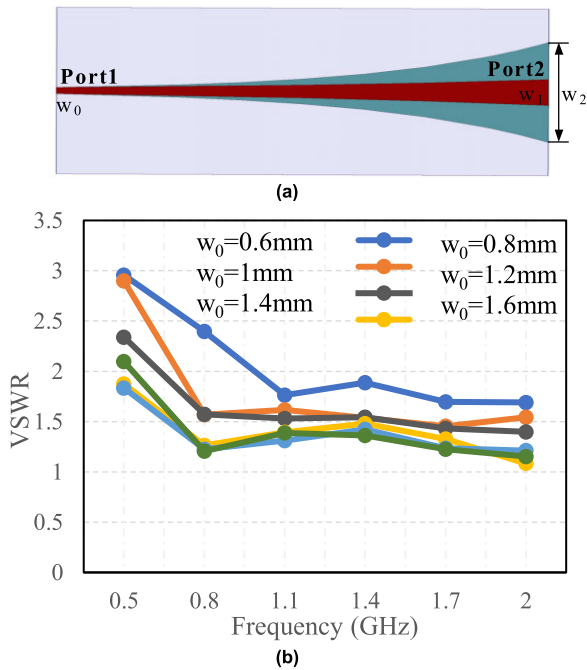


FIGURE 6. Microstrips Balun (a) and its VSWR at different w_0 (b).

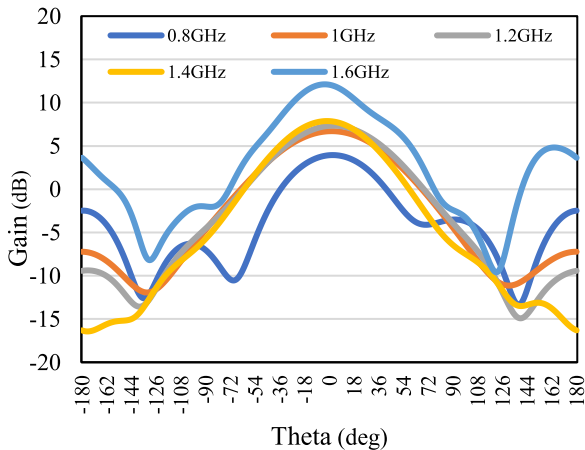


FIGURE 7. Radiation pattern at four frequencies.

1.4 mm, respectively, to make sure that the antenna’s VSWR is lower than 2.0 in the frequency ranging from 0.5 to 2.0 GHz and thus, improved impedance mismatch performance and high energy transmission efficiency when using impulsive voltages for PD tests.

Frequency gain is another parameter reflecting the energy transmission performance of antenna used for PD measurements. Higher gain means that more energy from PD activities will be received. The energy radiation pattern at a frequency from 0.8 to 1.6 GHz is reported in Figure 7, indicating that the antenna has unidirectional radiation characteristics in the operating frequency band. Antenna gain will increase from around 3.9 to 12.0 dB when the frequency is increased from 0.5 to 1.6 GHz.

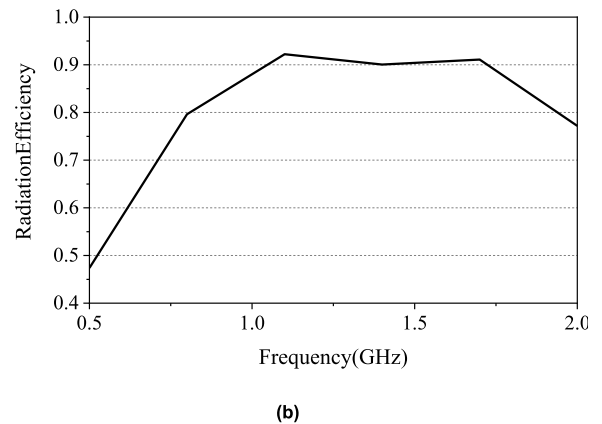
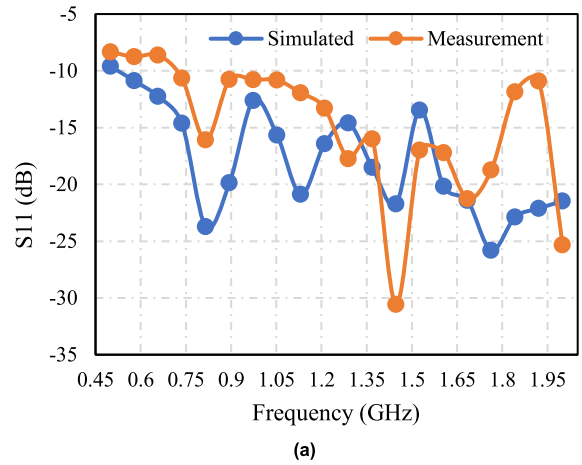


FIGURE 8. Field measurement and simulation S_{11} (a) and the near field radiation efficiency of the antenna varies with frequency (b).

E. ANALYSIS OF S PARAMETER AND ELECTRICAL FIELD DISTRIBUTION

Antenna’s input-output relation between ports can be described using S-parameter. S-parameter is tested by a vector network analyzer (Agilent E8362B). The measurement and simulation results of S_{11} vs. frequency of the ASA are shown in Figure 8a. The measured return loss of the antenna is higher than -9.54 dB in the range of 0.5 to 0.7 GHz. In comparison, the return loss is lower than -10 dB in the range of 0.7 to 2 GHz, indicating that the designed antenna’s performance is acceptable in the working frequency from 0.5 to 2.0 GHz [12], [13]. The near field radiation efficiency of antenna simulated is shown in the figure 8b, it can be seen that the antenna radiation efficiency is higher than 70% in the range of 0.5-1.875GHz, including the receiving frequency domain of PD, which can effectively receive PD information.

Antenna electric field distribution can reflect the antenna’s energy concentration performance. Antenna’s electric field distribution at 0.5 GHz, 1 GHz, 1.5 GHz, and 2 GHz frequency were calculated, as can be seen in Figures 9a, 9b, 9c, 9d. In order to receive the spectrum energy of PD pulse in a wider range, the optimal design of ASA is obtained by

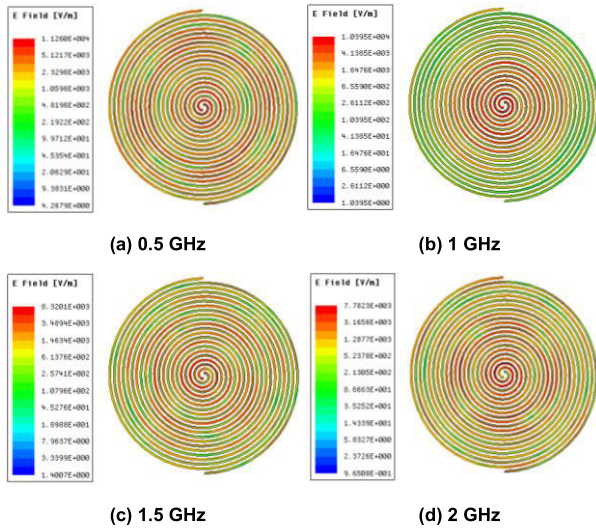


FIGURE 9. (a, b, c, d) Electric field distribution of ASA.

simulation analysis. HFSS was used to simulate and analyze the electric field distribution and three-dimensional gain diagrams of antenna at 0.5, 1, 1.5 and 2 GHz, which verified the effectiveness of the antenna frequency band detected by PD insulation under square pulse voltage.

It can be seen from Figure 9 that the antenna has a uniform electric field distribution at different operating frequencies. Results show that the antenna receives discharge signal effectively in the working frequency band. Combined with the three-dimensional (3-D) gain results at different frequencies, the 3-D gain patterns at different frequencies as shown in Figure 10 indicate that the ASA has an excellent directionality and, thus, it can receive high-gain partial discharge energy from one direction.

III. EXPERIMENTAL VERIFICATION OF THE ANTENNA AND ANALYSIS

A. EXPERIMENTAL PLATFORM

A repetitive impulsive voltage generator with variable parameters was firstly built to perform PD tests on inverter-fed motor insulation under impulse voltages. The voltage parameter (e.g., magnitude, rise time, duty cycle and frequency) of the voltage converters feeding the motors vary depending on many factors such as the motor properties and on-field configurations. Accordingly, the impulse voltage generator used for insulation tests for inverter-fed motor should have adjustable parameters accordingly to the IEC 60034-18-41 and 60034-18-42. A novel generator that can produce repetitive impulse voltage with adjustable parameters is reported in previous work [12]. PD tests resorting to the designed antenna were carried out at impulsive voltages produced by the generator with voltage parameters listed in Table 2.

For PD features or low voltage motor study, turn to turn insulation models were commonly used as specimens. The twisted pairs used in this study are made up of two enameled wires insulated by polyamide-imide material [37].

TABLE 2. Voltage parameters of the impulsive generator used for PD tests.

Voltage parameters	Value
Rise-fall time	20-1000 ns
Duty cycle	50%
Frequency	50Hz
dV/dt	10V/ns, 12V/ns, 14V/ns, 16V/ns, 18V/ns, 20V/ns,
Voltage	2kV, 2.4kV, 2.8kV, 3.2kV, 3.6kV, 4kV

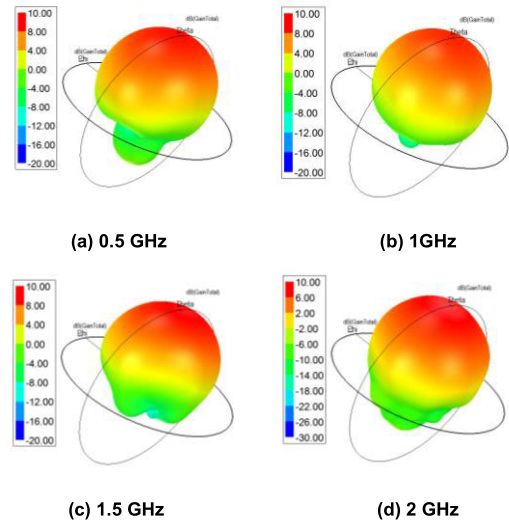


FIGURE 10. 3-D Radiation patterns.

The experimental platform of the tests is sketched in Figure 11a. The designed antenna (see Figure 12) was put and fixed in a box made up of Acrylonitrile-Butadiene-Styrene, and a high-pass filter with a cutting frequency of 399 MHz was connected to an antenna for the removal of low-frequency interference generated switching activities of power devices. And the filtered PD signal was connected to an oscilloscope with a sampling rate of up to 16 GHz and a bandwidth of 2.5 GHz. The PD test system under repetitive square wave voltages is shown in Figure 11b,c. Typical PD pulse received by the antenna and Time-frequency spectrum of PD are reported in Figure 13a and Figure 13b respectively. It can be known from Figure 3 that the background noise amplitude is around 4 mV, and the PD amplitude is higher than 20 mV. In Figure 13, the amplitude of the PD received by the designed antenna can reach 900 mV.

Therefore, the SNR of the PD detection has increased from 5 to 45 by using the new antenna with optimized parameters.

B. PD EXPERIMENTS UNDER IMPULSIVE VOLTAGES WITH DIFFERENT VOLTAGES

To find the PDIV of the specimens, preliminary tests were performed with repetitive impulsive voltages. PDIV peak-peak voltage was around 1.6 kV (peak to peak) and thus, bipolar impulse voltage with six different rise time keeping

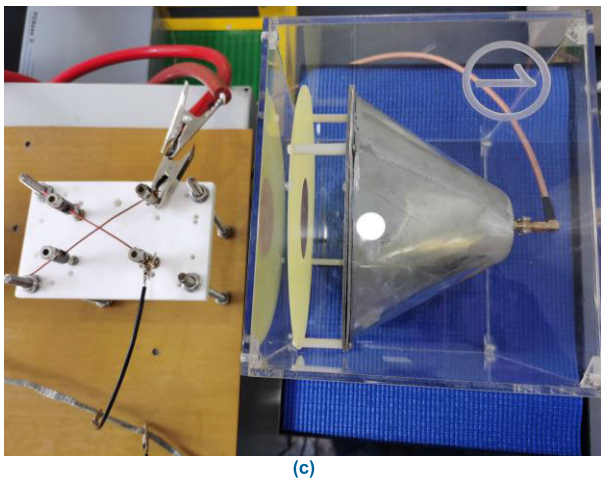
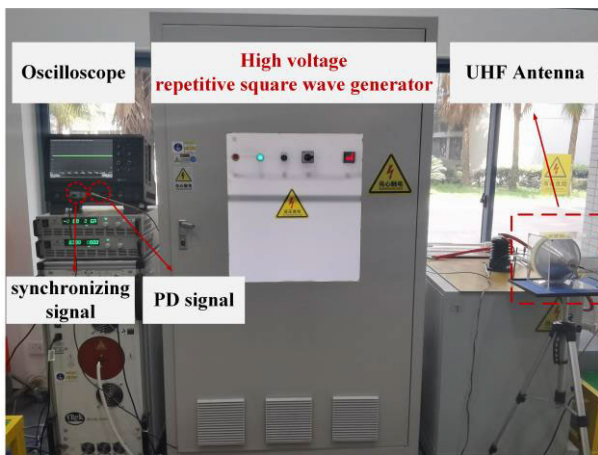
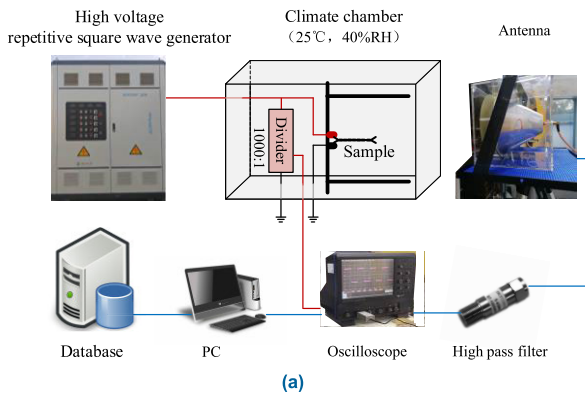


FIGURE 11. PD test system with detector (a), physical diagram of test platform (b) and Sample placement position (c).

magnitude at 2.0 kV was used to investigate the PD features. To obtain PD pulses statistical features, in each test a minimum of 500 cycles were saved for later analysis. The time between PD occurring and the nearest zero impulse voltage is defined as the PD delay time. The box plots of PD magnitude and delay time (along with the 95% confidence interval of the mean) are reported in Figure 15. Higher impulse voltage gives rise to PD with higher magnitude and shorter delay time. The influence of voltage magnitude on PD frequency energy

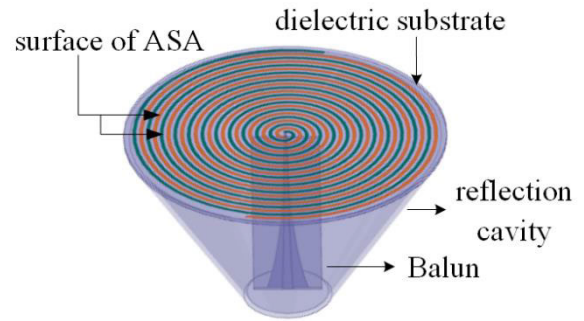


FIGURE 12. Three-dimensional antenna.

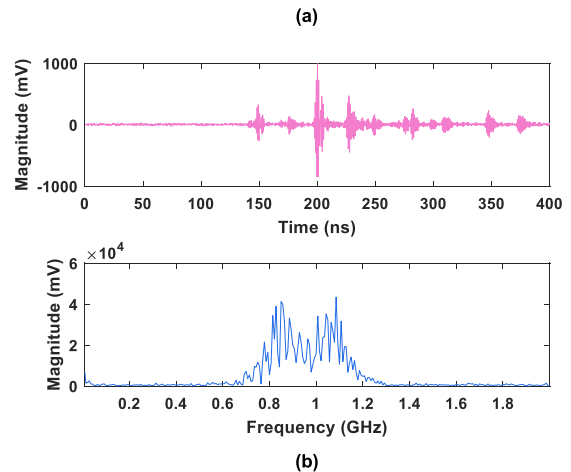
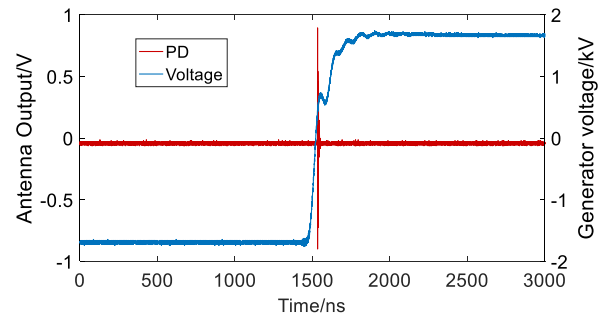


FIGURE 13. (a) Typical PD pulse received by the antenna (b) PD test results in time and frequency domain.

distribution was also analyzed and reported in Figure 15. It can be observed that the PD pulses received by the designed antenna distribute in the frequency range from 0.5 to 2.0 GHz. And, it is interesting to note that, impulse voltages with higher magnitude tends to induce PD having more energy from 1.5 to 2.0 GHz. We have reported that short rise time can give rise to PD with higher magnitude in the time domain and energy distribution in the frequency domain on the basis of PD measurements conducted at impulse voltages with rising time from 200 ns to 16 μ s keeping the impulse voltage at 3.5 kV [13]. Although the PD tests reported in Figure 14 were carried out at impulse voltages with same rise time, the voltage slew rate (dv/dt) can increase with increasing voltage magnitude and thus, lead to PD pulses with increasing energy distribution at a frequency from 1.5 to 2.0 GHz.

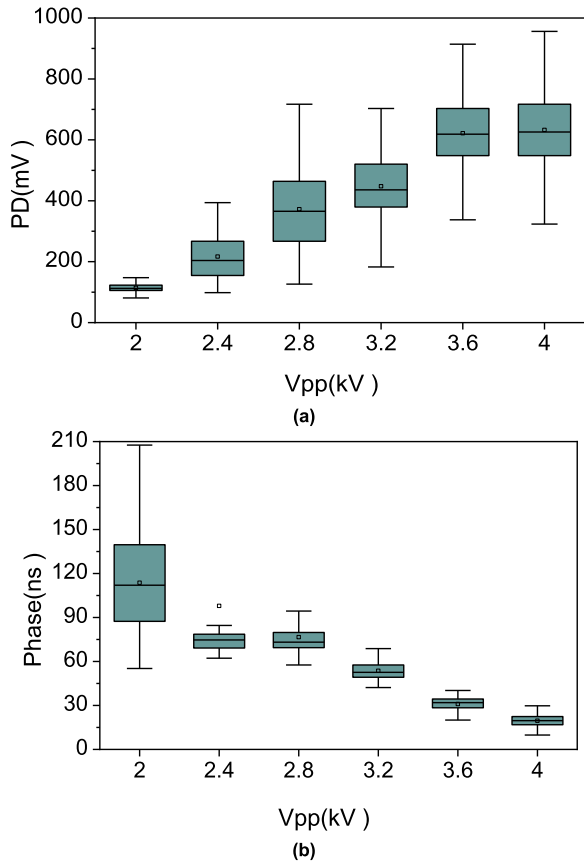


FIGURE 14. PD amplitude (a) and phase distribution (b) at different voltage magnitude.

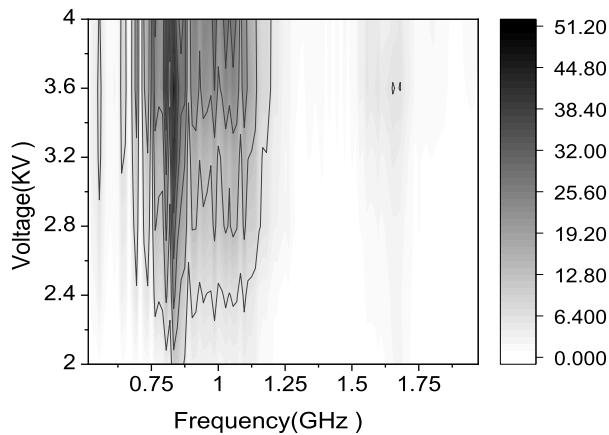


FIGURE 15. PD spectrum at different voltage magnitude.

C. PD TEST AT DIFFERENT DISTANCE

The PD signals are investigated at ASA distances varying from 10 to 45 cm (10, 15, 20, 25, 30, 35, 40, 45cm), which received by the antenna as indicators to explore the time domain characteristics of PD and study the propagation characteristics of PD signals. The rise time, duty cycle, frequency, and peak-to-peak voltage of impulsive voltages were kept at 200 ns, 50%, 50 Hz and 2.5 kV, respectively. The obtained PD energy spectra at different

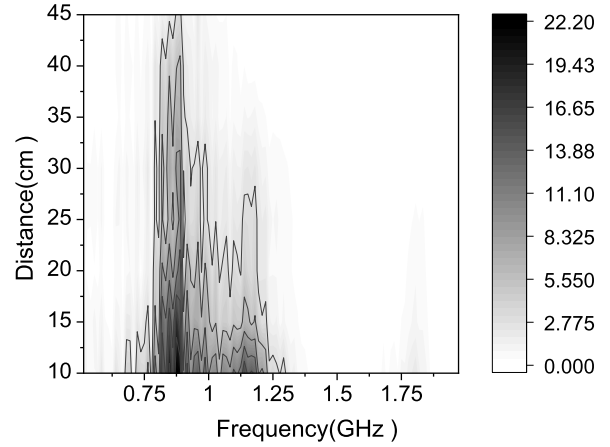


FIGURE 16. PD spectrum vs. test distance.

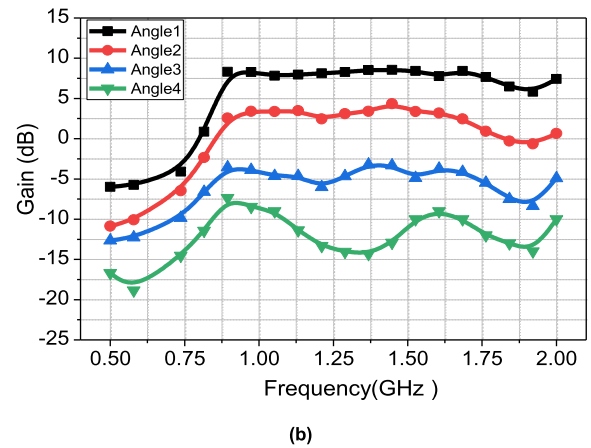
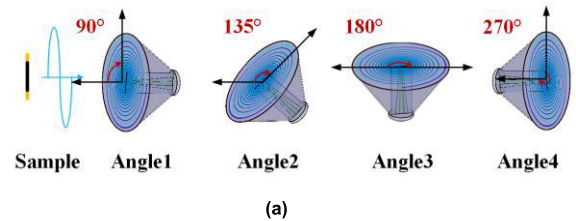


FIGURE 17. (a) Measuring angle of ASA (b) Simulated peak gain at different placing angles.

distance is reported in Figure 16. It can be observed that most energy of the PD pulses distributes from 0.6 GHz to 1.25 GHz. And, the PD magnitude and its frequency content decrease significantly with increasing distance, especially in the high-frequency range from 1 to 1.2 GHz. When the test distance reaches 30 cm, the energy in frequency domain higher than 1 GHz reduce obviously to a lower level. When the test distance is longer than 30 cm, most of the PD energy ranging from 1.0 GHz to 2.0 GHz will disappear. The above results indicate that, the antenna can have the best performance when the distance between the test object and the antenna is within 15 cm. The shorter distance between the antenna and discharge location, the more near-field energy from PD events can be received and thus, better gain performance.

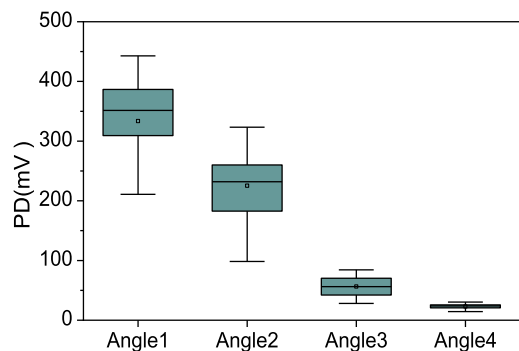


FIGURE 18. Peak magnitude of PD at different placing angles.

D. PD TEST AT DIFFERENT PLACING ANGLES

The 3-D gain direction simulation results reported in Figure 10 show that the ASA is omnidirectional, i.e. the antenna can receive electromagnetic wave signals from all directions with different gain. The antenna cannot be installed in the direction with the best gain features when performing PD measurements. Therefore, the influence of antenna direction on PD gain features should be investigated to verify the performance of the designed antenna. The frequency, peak-to-peak voltage, duty cycle, and rise time were maintained at 50 Hz, 2.5 kV, 50%, and 1000 ns, respectively. The antenna in this paper is placed at four different angles as demonstrated in Figure 17a. PD amplitude vs. placing angles was reported in the box charts of Figure 18.

The effective signal receiving area of the antenna gradually decreases by increasing the angle between the antenna receiving surface and the sample placement plane, which leads to lower down the PDs magnitude. When the angle between the direction of a signal coming wave and the antenna receiving surface is between 90° and 270° , the antenna can receive PD signals with high energy efficiency, which confirms the omnidirectional capability of the designed antenna. Besides, the PD events with the highest amplitude were acquired by the antenna at the angle of 1, which is consistent with the gain simulation results reported in Figure 17b. Under the condition of Angle 3, the PD signals received by the antenna have considerable energy losses because the overall gain level is the lowest relative to Angle 1 and 2.

E. ENVELOPE DETECTION

When the PD signal with spectrum bandwidth up to GHz is collected, the data acquisition device is highly required and will obtain huge data. The PD envelope signal obtained by the envelope detection circuit has a similar shape as the original signal, and the energy distribution in the frequency domain is transformed from 0.5 to 2.0 GHz to frequency range lower than 50 MHz. And the sampling rate of 100 MHz can accurately collect the peak value and phase of partial discharge according to the sampling theorem. Therefore, the bandwidth, sampling rate requirement of the acquisition system and data storage space of hardware can be largely

reduced. The envelope detection of PD signals is carried out by selecting, $R = 100 \Omega$, $C = 1 \text{ pF}$, the detailed explanation is mentioned in reference [39], [40].

F. ANALYSIS

The novelty of this work is the optimization of the designed antenna towards the PD detection at high frequency and short rise time square impulse voltage waveform while considering the distance and angles of antenna effects on the output signal quality. The performance of the designed antenna is verified under different placement distances and angles by changing the frequency and amplitude of the impulse voltage input signal during PD detection as shown in Table 3. Based on the above parameters, we obtained the following conclusions: The frequency-domain energy of PD under square wave impulse voltage is mainly distributed in the range of 0.6 to 1.8 GHz. With the increase of input voltage amplitude, the frequency-domain energy distribution of PD changes to around 1.5 to 1.8 GHz. The results have shown that the higher part of the frequency-domain energy distribution of PD attenuates more severely with distance. The electromagnetic energy of PD decays nonlinearly with the increase of propagation distance. When the antenna is close to the discharge point, the higher part of the frequency-domain energy signal was detected by the antenna at 1.8 GHz. We have observed that keeping the discharge point distance $\leq 30 (\pm 5)$ cm (the wavelength corresponding to the maximum operating frequency of the antenna) can ensure that the test results have a high signal-to-noise ratio and signal integrity.

To reduce the hardware expenditures, the envelop detection circuit was designed to convert the UHF amplitude modulated signal into the low frequency bandwidth signal having the same shape as the original signal. In this envelope detection the energy distribution in frequency domain is transformed from 0.5 to 2 GHz to below 50 MHz as shown in Table 4. PD peak is amplified, but the pulse phase remains the same, detector output can be directly connected to PD processing system with MHz bandwidth, which makes PD detection more diversified under repetitive impulsive voltages with fast rise times. The sampling rate of 100 MHz can accurately collect the peak value and phase of partial discharge according to the sampling theorem. Therefore, the bandwidth, sampling rate requirement of the acquisition system and data storage space of hardware can be largely reduced.

IV. CONCLUSION

The PD tests under impulsive voltages are difficult and complex mainly because the disturbance generated by switching on & off of power devices and the conventional test methods such as direct coupling using measurement impedance and HFCT are insufficient. This work aims to report our experience on the PD measurements under impulsive voltages resorting to the UHF technique. The UHF technique shows its potential capacity when detecting PD under repetitive impulsive voltages with short rise times and high frequency.

TABLE 3. Influence of the parameters of designed antenna on PD detection.

Variable	UHF PD spectrum (GHz)		Envelope Detection PD spectrum (MHz)	PD amplitude	PD phase
	Low frequency	High frequency		as the variable increases	
Distance	0.7-1.25	1.5-1.8	<50	attenuation	no
Voltage	0.5-1.25	1.5-1.8	<50	increase	attenuation

TABLE 4. Comparison of proposed method of detection.

PD detection technology	PD spectrum	Voltage	Characteristics	Widespread use
UHF	0.5-2 GHz	Impulsive voltage	High SNR and high detection sensitivity	Detection and time-frequency analysis of PD in laboratory and on-site
HFCT [43,44]	<20 MHz	Sinusoidal voltage	High pulse resolution, low SNR, easy to be affected by interference	PD detection under sine in laboratory
Envelop detection	<50MHz	Impulsive voltage	Amplifier and demodulation the sampling rate and bandwidth of the signal acquisition system are required to be low	PD on-line detection

Number of PD tests performed under repetitive impulsive voltages with different parameters (i.e., rise time, from 50 ns to 100 ns, frequency from 50 Hz to 5 kHz) by using the designed antenna on the turn to turn insulation for inverter-fed motor concluded that:

1. The sensitivity of the UHF sensor affects the accuracy of PD acquisition and the reliability of insulation evaluation. The repetitive impulsive voltage parameters such as rise time, duty cycle and frequency can have a significant influence on the amplitude, phase, and time-frequency distribution of PD signals. Therefore, we have considered these parameters carefully and optimized the antenna parameters to improve the sensitivity of the detection system.
2. The frequency domain energy of PD signals from motor insulation under impulsive voltage is mainly distributed in the range of 0.6 to 1.8 GHz. By increasing the amplitude and frequency of input impulsive voltage, the range of partial discharge energy spectrum is also enlarged around 1.5 to 1.8 GHz.
3. The PD electromagnetic energy under repetitive impulse voltage decays nonlinearly with the increase of propagation distance. When the antenna is close to the discharge point, the high-frequency signal energy detected by the antenna is mainly at 1.8 GHz and the high-frequency distribution of partial discharge energy attenuates more severely with distance. Therefore, under the premise of satisfying the safety test, selecting the test distance below 15 cm (the wavelength corresponding to the maximum operating frequency of the antenna) can ensure that the test results have a high SNR ratio and signal integrity.

REFERENCES

- [1] M. Tozz, A. Cavallini, and G. Montanari, "Monitoring off-line and on-line PD under impulsive voltage on induction motors—Part I: Standard procedure," *IEEE Elect. Insul. Mag.*, vol. 26, no. 4, pp. 16–26, Jul. 2010.
- [2] M. J. Melfi, "Low-voltage PWM inverter-fed motor insulation issues," *IEEE Trans. Ind. Appl.*, vol. 42, no. 1, pp. 128–133, Jan. 2006.
- [3] J. C. G. Wheeler, "Effects of converter pulses on the electrical insulation in low and medium voltage motors," *IEEE Elect. Insul. Mag.*, vol. 21, no. 2, pp. 22–29, Mar. 2005.
- [4] S. Akram, Y. Yang, X. Zhong, S. Bhutta, G. Wu, J. Castellon, and K. Zhou, "Influence of nano layer structure of polyimide film on space charge behavior and trap levels," *IEEE Trans. Dielectr. Electr. Insul.*, vol. 25, no. 4, pp. 1461–1469, Aug. 2018.
- [5] C. Abadie, T. Billard, and T. Lebey, "Partial discharges in motor fed by inverter: From detection to winding configuration," *IEEE Trans. Ind. Appl.*, vol. 55, no. 2, pp. 1332–1341, Mar. 2019.
- [6] S. Akram, G. Wu, G. Gao, and Y. Liu, "Effect of surface discharge on nano filled polyimide film under square voltage," in *Proc. IEEE Electr. Insul. Conf. (EIC)*, Aug. 2015, pp. 226–229.
- [7] S. Akram, G. Wu, G. Gao, and Y. Liu, "Cavity and interface effect of PI-film on charge accumulation and PD activity under bipolar pulse voltage," *J. Electr. Eng. Technol.*, vol. 10, no. 5, pp. 2089–2098, Sep. 2015.
- [8] S. Akram, G. Gao, Y. Liu, J. Zhu, and G. Wu, "Degradation mechanism of Al₂O₃ nano filled polyimide film due to surface discharge under square impulse voltage," *IEEE Trans. Dielectr. Electr. Insul.*, vol. 22, no. 6, pp. 3341–3349, Dec. 2015.
- [9] *Rotating Electrical Machines—Part 18-41: Qualification and Type Tests for Type 1 Electrical Insulation Systems Used in Rotating Electrical Machines Fed From Voltage Converters*, Standard IEC 60034-18-41, 2006.
- [10] *Rotating Electrical Machines—Part 18-42: Qualification and Acceptance Tests for Partial Discharge Resistant Electrical Insulation Systems (Type II) Used in Rotating Electrical Machines Fed From Voltage Converters*, Standard IEC 60034-18-42 Ed 1.0, 2008.
- [11] S. Akram, P. Wang, M. T. Nazir, K. Zhou, M. S. Bhutta, and H. Hussain, "Impact of impulse voltage frequency on the partial discharge characteristic of electric vehicles motor insulation," *Eng. Failure Anal.*, vol. 116, Oct. 2020, Art. no. 104767.
- [12] P. Wang, H. Xu, J. Wang, and A. Cavallini, "The influence of repetitive square wave voltage duty cycle on partial discharge statistics and insulation endurance," in *Proc. Int. Conf. Condition Monitor. Diagnosis (CMD)*, Xi'an, China, Sep. 2016, pp. 274–277, doi: 10.1109/CMD.2016.7757808.
- [13] P. Wang, A. Cavallini, G. C. Montanari, and G. Wu, "Effect of rise time on PD pulse features under repetitive square wave voltages," *IEEE Trans. Dielectr. Electr. Insul.*, vol. 20, no. 1, pp. 245–254, Feb. 2013.
- [14] G. C. Stone, H. G. Sedding, and C. Chan, "Experience with online partial-discharge measurement in high-voltage inverter-fed motors," *IEEE Trans. Ind. Appl.*, vol. 54, no. 1, pp. 866–872, Jan. 2018.
- [15] M. Kaufhold, G. Borner, M. Eberhardt, and J. Speck, "Failure mechanism of the interturn insulation of low voltage electric machines fed by pulse-controlled inverters," *IEEE Elect. Insul. Mag.*, vol. 12, no. 5, pp. 9–16, Sep. 1996.
- [16] G. N. Wu, Y. Yang, X. Zhong, S. Akram, X. T. Zhang, X. H. Wu, and J. Zhu, "Research progress of key characteristics and nano-modification of insulating material for inverter-fed traction motor," *Insulating Mater.*, vol. 9, p. 4, 2016.

- [17] A. Cavallini, G. C. Montanari, D. Fabiani, and M. Tozzi, "The influence of PWM voltage waveforms on induction motor insulation systems: Perspectives for the end user," in *Proc. 8th IEEE Symp. Diag. Electr. Mach., Power Electron. Drives*, Bologna, Italy, Sep. 2011, pp. 288–293, doi: [10.1109/DEMPED.2011.6063638](https://doi.org/10.1109/DEMPED.2011.6063638).
- [18] W. Zhou, P. Wang, Z. Zhao, Q. Wu, and A. Cavallini, "Design of an archimedes spiral antenna for PD tests under repetitive impulsive voltages with fast rise times," *IEEE Trans. Dielectr. Electr. Insul.*, vol. 26, no. 2, pp. 423–430, Apr. 2019.
- [19] K. Kimura, S. Okada, and M. Hikita, "Electromagnetic wave in GHz region of PD pulses under short rise time repetitive voltage impulses," in *Proc. Int. Symp. Electr. Insulating Mater. (ISEIM)*, Mie, Japan, Sep. 2008, pp. 633–636, doi: [10.1109/ISEIM.2008.4664487](https://doi.org/10.1109/ISEIM.2008.4664487).
- [20] Y. Gong, P. Wang, W. Zhou, J. Zhang, and A. Cavallini, "A novel archimedes spiral antenna used for PD measurement at repetitive square wave voltages," in *Proc. IEEE Conf. Electr. Insul. Dielectr. Phenomena (CEIDP)*, Cancun, Mexico, Oct. 2018, pp. 502–505, doi: [10.1109/CEIDP.2018.8544893](https://doi.org/10.1109/CEIDP.2018.8544893).
- [21] J. Li, X. Han, Z. Liu, and X. Yao, "A novel GIS partial discharge detection sensor with integrated optical and UHF methods," *IEEE Trans. Power Del.*, vol. 33, no. 4, pp. 2047–2049, Aug. 2018.
- [22] S. Okada, K. Fukunaga, K. Yamaguchi, S. Ohtsuka, K. Kimura, and M. Hikita, "Comparison of electromagnetic wave, light intensity and electric charge of PD on crossed magnet wires under repetitive impulses," in *Proc. Annu. Rep. Conf. Electr. Insul. Dielectr. Phenomena*, Quebec, QC, Canada, Oct. 2008, pp. 391–394, doi: [10.1109/CEIDP.2008.4772812](https://doi.org/10.1109/CEIDP.2008.4772812).
- [23] F. Guastavino, A. Dardano, and E. Torello, "Measuring partial discharges under pulsed voltage conditions," *IEEE Trans. Dielectr. Electr. Insul.*, vol. 15, no. 6, pp. 1640–1648, Dec. 2008.
- [24] S. Park and K.-Y. Jung, "Design of a circularly-polarized UHF antenna for partial discharge detection," *IEEE Access*, vol. 8, pp. 81644–81650, Apr. 2020.
- [25] Y. Qi, Y. Fan, G. Bing, R. Jia, W. Sen, S. Wei, and A. Jadoon, "Design of ultra-wide band metal-mountable antenna for UHF partial discharge detection," *IEEE Access*, vol. 7, pp. 60163–60170, Apr. 2019.
- [26] N. Hayakawa, H. Inano, and H. Okubo, "Partial discharge inception characteristics by different measuring methods in magnet wire under surge voltage application," in *Proc. Annu. Rep.-Conf. Electr. Insul. Dielectr. Phenomena*, Vancouver, BC, Canada, 2007, pp. 128–131, doi: [10.1109/CEIDP.2007.4451515](https://doi.org/10.1109/CEIDP.2007.4451515).
- [27] N. Hayakawa, H. Inano, Y. Nakamura, and H. Okubo, "Time variation of partial discharge activity leading to breakdown of magnet wire under repetitive surge voltage application," *IEEE Trans. Dielectr. Electr. Insul.*, vol. 15, no. 6, pp. 1701–1706, Dec. 2008.
- [28] Y. Wang, J. Wu, W. Chen, T. Zhu, and Y. Wang, "Design of a UHF antenna for partial discharge detection of power equipment," *J. Sensors*, vol. 2014, pp. 1–8, Oct. 2014.
- [29] H. Muto, Y. Kaneda, H. Aoki, and O. Hamamoto, "On-line PD monitoring system for rotating machines using narrow band detection of EM wave in GHz range," in *Proc. Int. Conf. Condition Monitor. Diagnosis*, Apr. 2008, pp. 1093–1096.
- [30] F. Ashari and U. Khayam, "Design and fabrication of Vivaldi antenna as partial discharge sensor," in *Proc. 4th Int. Conf. Electr. Veh. Technol. (ICEVT)*, Oct. 2017, pp. 76–78.
- [31] J. Li, P. Wang, T. Jiang, L. Bao, and Z. He, "UHF stacked Hilbert antenna array for partial discharge detection," *IEEE Trans. Antennas Propag.*, vol. 61, no. 11, pp. 5798–5801, Nov. 2013.
- [32] G. Robles, J. M. Martinez-Tarifa, M. V. Rojas-Moreno, R. Albarracin, and J. Ardila-Rey, "Antenna selection and frequency response study for UHF detection of partial discharges," in *Proc. IEEE Int. Instrum. Meas. Technol. Conf.*, Graz, Austria, May 2012, pp. 1496–1499, doi: [10.1109/I2MTC.2012.6229440](https://doi.org/10.1109/I2MTC.2012.6229440).
- [33] J. J. H. Wang, C. J. Stevens, and D. J. Triplett, "Ultra-wideband omnidirectional conformable low-profile mode-0 spiral-mode microstrip (SMM) antenna," in *Proc. IEEE Antennas Propag. Soc. Int. Symp.*, Washington, DC, USA, Jul. 2005, pp. 549–552, doi: [10.1109/APS.2005.1552310](https://doi.org/10.1109/APS.2005.1552310).
- [34] D. Fabiani, A. Cavallini, and G. C. Montanari, "A UHF technique for advanced PD measurements on inverter-fed motors," *IEEE Trans. Power Electron.*, vol. 23, no. 5, pp. 2546–2556, Sep. 2008.
- [35] R. He, H. Zhang, C. H. See, Y. Su, Y. Ma, D. Kong, X. Zhu, and R. Abd-Alhameed, "A 1×8 linear ultra-wideband phased array with connected dipoles and hyperbolic microstrip baluns," *IEEE Access*, vol. 6, pp. 52953–52968, Dec. 2018.
- [36] T. Xia, S. Yang, and Z. Nie, "Design of a tapered balun for broadband arrays with closely spaced elements," *IEEE Antennas Wireless Propag. Lett.*, vol. 8, pp. 1291–1294, 2009.
- [37] S. Akram, M. T. Nazir, J. Castellon, S. Agnel, K. Zhou, and M. S. Bhutta, "Preparation and distinguish dielectric properties of multi-layer nanoparticles-based polyimide films," *Mater. Res. Express*, vol. 6, no. 12, Dec. 2019, Art. no. 125092.
- [38] D. Wienold, U. Lühring, and F. Jenau, "Detection and distinction of partial discharges in air at DC voltage by using a non-conventional approach in the high-frequency range," in *Proc. IEEE Int. Conf. Environ. Electr. Eng. IEEE Ind. Commercial Power Syst. Eur. (EEEIC / I&CPS Europe)*, Jun. 2017, pp. 1–5.
- [39] A. Zaeni and U. Khayam, "Designing, simulating, and manufacturing envelope detector to analyze partial discharge waveform," in *Proc. Joint Int. Conf. Electr. Veh. Technol. Ind., Mech., Electr. Chem. Eng. (ICEVT IMECE)*, Nov. 2015, pp. 91–94.
- [40] A. Zaeni and U. Khayam, "Enveloping partial discharge signal using direct interpolation method," in *Proc. 4th Int. Conf. Electr. Veh. Technol. (ICEVT)*, Oct. 2017, pp. 65–70.
- [41] P. Wang, G. C. Montanari, and A. Cavallini, "Partial discharge phenomenology and induced aging behavior in rotating machines controlled by power electronics," *IEEE Trans. Ind. Electron.*, vol. 61, no. 12, pp. 7105–7112, Dec. 2014.

...